English
Research Express@NCKU Volume 28 Issue 6 - February 13, 2015
[http://research.ncku.edu.tw/re/articles/e/20150213/4.html]

Dislocation reduction through nucleation and growth selectivity of metalorganic chemical vapor deposition GaN

Wei Zhang[1], Peichi Liu[1], Biyun Jackson[1], Tianshu Sun[2], Shyh-Jer Huang[3], Hsiao-Chiu Hsu[3], Yan-Kuin Su[4], Shoou-Jinn Chang[3,*], Lei Li[5], Ding Li[5], Lei Wang[5], XiaoDong Hu[5], Y. H. Xie[1]

[1] Department of Materials Science and Engineering, University of California Los Angeles, California 90095, USA

[2] Department of Physics, University of Maryland college park, Maryland 20742, USA

[3] Advanced Optoelectronic Technology Center and Institute of Microelectronics and Department of Electrical Engineering, National Cheng Kung University, Tainan 701, Taiwan

[4] Department of Electrical Engineering, Kun Shan University of Technology, Yung-Kang, Tainan 710, Taiwan

[5] State Key Laboratory for Artificial Microstructure and Mesoscopic Physics, School of Physics, Peking University, Beijing 100871, China

changsj@mail.ncku.edu.tw

Journal of Applied Physics, Vol. 113, p. 144908, 2013

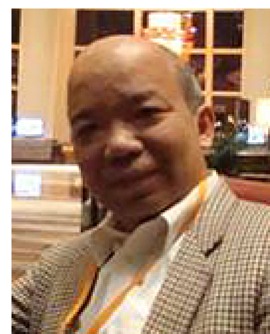

GaN and III-nitride alloys have emerged as surpassingly useful materials for the fabrication of green-to-ultraviolet light-emitting diodes, [1–3] laser diodes[4] and high-power, high-efficiency transistor devices[5] due to their widely tunable bandgap. Heteroepitaxial growth of GaN on Si, sapphire and/or SiC, is an important and fundamental technological challenge because of the lack of intrinsic GaN substrates. However, owning to the approximately 17% lattice mismatch, the associated density of dislocations is typically 10^8-10^{10} cm^{-2} in un-patterned GaN epi-layers. The high density of dislocations greatly limits the application potential of GaN-based devices. [6–8] In this study, we report a novel mask with serpentine shaped channels that requires only one epitaxial growth step for obtaining GaN films with low dislocation density of 10^5 cm^{-2}.

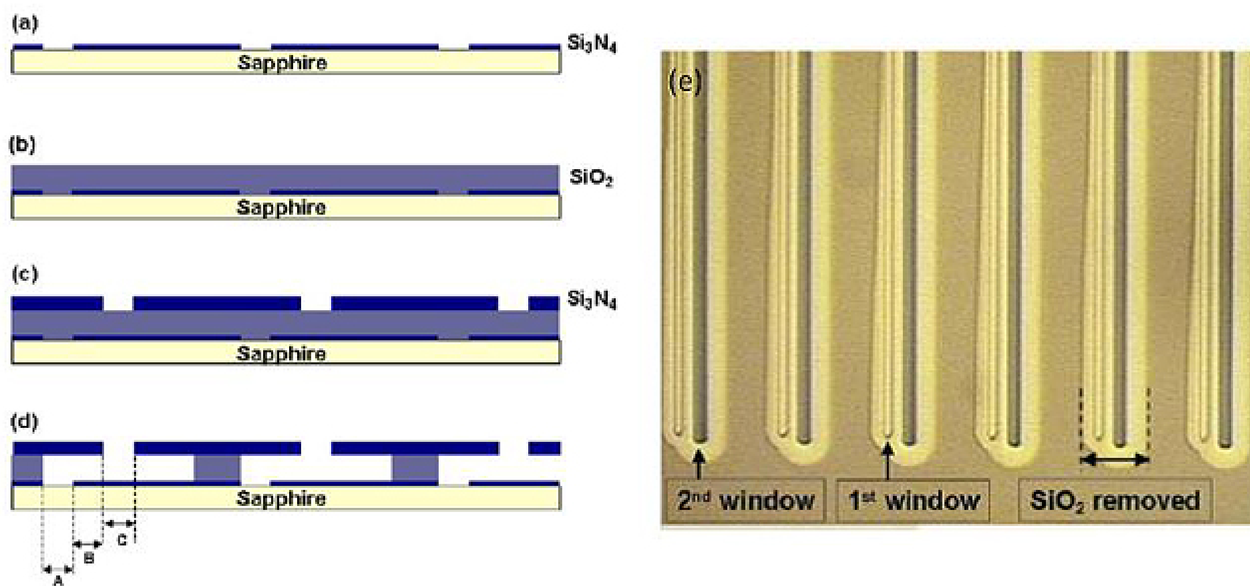

Fig. 1 (a)-(d) schematic process flow of the masked sapphire substrate with serpentine channel (cross-sectional

view). A, B and C are dimensions of 1st opening, channel length and 2nd opening; (e) plan-view optical microscopy image of the masked sapphire substrate.

Figure 1 is a schematic process flow of the masked sapphire substrate with the serpentine channel structure. First, a thin Si_3N_4 was deposited on sapphire substrate by low pressure chemical vapor deposition (LPCVD), followed by the standard photolithography and reactive-ion etching to define the 1st level of windows with a periodicity of 12 µm as shown in Fig. 1(a). Next, SiO_2 was deposited on the 1st layer by LPCVD as shown in Fig. 1(b) and then a thicker Si_3N_4 layer was deposited by LPCVD. Conventional photolithography was employed to define the 2nd level of windows with the same periodicity and orientation (Fig. 1(c)) as the 1st level but with a lateral phase shift to form the serpentine crosssectional channel. As last, isotropic etching was carried out to remove SiO_2 using BOE in the intermediate layer, stopping when the sapphire surface was exposed in the window regions of the first Si_3N_4 layer as shown in Fig. 1(d). Fig. 1(e) shows the plan-view optical microscopy image of the masked substrate.

Figures 2(a) - 2(e) shoe theCross sectional TEM. Figures 2(b) - 2(e) are dark-field STEM images, which represent the detailed evolution of dislocations at four different typical regions of the serpentine channel corresponding to the regions marked as A, B, C, and D in Fig. 2(a), respectively. The channel length shown in Fig. 2(a) is shorter than our original design due to the undesired but somehow inevitable fluctuations in the processing of different batch of samples. As shown in Fig. 2(b), all the dislocations generated at the GaN/sapphire interface were effectively blocked by the serpentine channel structure. It is the key innovative point to achieve significant dislocation reduction. Figures 2(c) and 2(d) show isolated dislocations running parallel to the GaN/sapphire interface. Such dislocations do not threaten the device performance fabricated at the top surface of the GaN layer similar to what has been shown for SiGe virtual substrates. No threading dislocations perpendicular to the interface are visible as GaN grows out as shown in Fig. 2(d). It is ascribed to the effectiveness of the serpentine channel in filtering dislocations. A coalescence front between adjacent stripes is shown in Fig. 2(e). As expected, it is obvious that high density of dislocations associated with the coalescent fronts, which highlights one of the key advantages of the innovative mask structure with serpentine channels. Figure 2(f) shows the top-view SEM image of GaN film after H_3PO_4+H_2SO_4 solution etching at 160℃ for 60min for etch pits density measurement. It can be observed a variation in etch pits density with the lowest value being around 4×10^5 cm^{-2}.

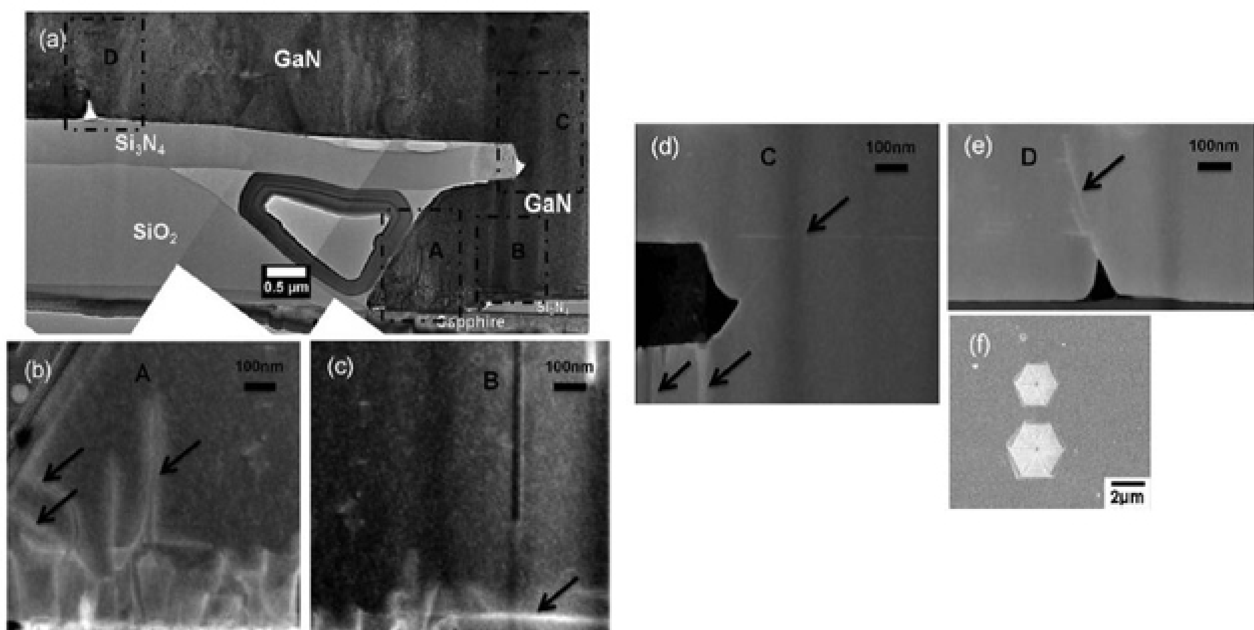

Fig. 2 (a) Cross-sectional bright-field TEM images of the GaN grown on the serpentine-channel masked sapphire substrate, and (b)-(e) dark-field STEM images of four typical regions marked as A, B, C, D in (a). Dislocations are marked by the arrows. (f) Top-view SEM images of the GaN film after H_3PO_4+H_2SO_4 solution etching at 160℃ for 60 min.

In summary, we developed an innovative serpentine masked structure to grow GaN epilayers. Very low dislocation density was achieved through further reduction by optimizing the growth condition. The presented serpentine masked structure did not need any regrowth process for obtaining low-defect-density GaN materials. The grown GaN films are promising for fabricating high-performance III–nitride-based devices.

Reference

1. S. Nakamura, T. Mukai, and M. Senoh, Appl. Phys. Lett. 64, 1687 (1994).
2. E. F. Schubert and J. K. Kim, Science 308, 1274 (2005).
3. S. Nakamura, N. Iwasa, M. Senoh, S. Nagahama, T. Yamada, and T. Mukai, Jpn. J. Appl. Phys., Part 2 34, L1332 (1995).
4. T. C. Lu, S. W. Chen, T. T. Wu, P. M. Tu, C. K. Chen, C. H. Chen, Z. Y. Li, H. C. Kuo, and S. C. Wang, Appl. Phys. Lett. 97, 071114 (2010).
5. U. K. Mishra, P. Parikh, and Y.-F. Wu, Proc. IEEE 90, 1022 (2002).
6. S. Nakamura, M. Senoh, S. Nagahama, N. Iwasa, T. Yamada, T. Matsushita, H. Kiyoku, Y. Sugimoto, T. Kozaki, H. Umemoto, M. Sano, and K. Chocho, Appl. Phys. Lett. 72, 211 (1998).
7. M. Furitsch, A. Avramescu, C. Eichler, K. Engl, A. Leber, A. Miler, C. Rumbolz, G. Brüderl, U. Strauß, A. Lell, and V. H€arle, Phys. Status Solidi A 203, 1797 (2006).
8. N. G. Weimann, L. F. Eastman, D. Dharanipal, H. M. Ng, and T. D. Moustakas, J. Appl. Phys. 83, 3656 (1998).
9. K. Hiramatsu, S. Itoh, H. Amano, and I. Akasaki, J. Cryst. Growth 115, 628 (1991).
10. Y. H. Xie, E. A. Fitzgerald, and P. J. Silverman, Mater. Sci. Eng. B 30, 201 (1995).

Copyright 2015 National Cheng Kung University